The International Journal of Geomechanics
Volume 1, Number 1, 21–39 (2001)

DEM Simulation of Particle Damage in Granular Media — Structure Interfaces

Richard P. Jensen , Michael E. Plesha , Tuncer B. Edil , Peter J. Bosscher, and Nabil Ben Kahla

Received August 10, 2000
Revision received December 11, 2000

Graduate Student, Geological Engineering Program, University of Wisconsin-Madison, Madison, WI 53706 (now at Sandia National Laboratories, Albuquerque, NM 87185-0751)

Professor, Dept. of Engineering Physics and Geological Engineering Program, University of Wisconsin-Madison, Madison, WI 53706

Professor, Dept. of Civil and Environmental Engineering and Geological Engineering Program, University of Wisconsin-Madison, Madison, WI 53706

Professor, Dept. of Civil and Environmental Engineering and Geological Engineering Program, University of Wisconsin-Madison, Madison, WI 53706

Visiting Scholar, Dept. of Engineering Physics, University of Wisconsin-Madison, Madison, WI 53706 (now at Ecole Nationale D'Ingénieurs De Gabès, Tunisia)

ABSTRACT. *Using the discrete element method (DEM) with clustering, a novel means of numerically modeling damage of particles is presented. Damage, such as grain crushing, is treated by allowing clusters to break apart according to a failure criterion based upon sliding work. If the accumulated work done on an individual DEM particle of a cluster exceeds a threshold, that particle is allowed to break from the cluster. A value for the critical energy density is determined by comparing the degree of particle breakage from numerical simulations to data from laboratory tests. Numerical simulations were also conducted to determine the impact of particle damage on interface behavior. It was found that a very distinct shear zone was evident when particle damage was considered and that this occurred without significant reduction of the maximum shear strength of the medium. Also, the degree of damage was shown to be related to the angularity of the clusters.*

Key Words: discrete element method (DEM), clustering, damage, grain crushing.

Acknowledgements and Notes. This research was performed with financial support from the National Science Foundation Grant CMS-9302281, U.S. Air Force Office of Scientific Research Grant MIPR-93-0031, and AASERT Grant F49620-94-1-0325.

 DOI: 10.1061/(ASCE)1532-3641(2001)1:1(21)
ISSN 1532-3641

I. Introduction

The interaction of solid surfaces with particulate media has been a topic of research for many years. Despite significant effort, a thorough understanding of the fundamental behavior of these interfaces, and development of quantitative models for macroscopic behavior, continues to be elusive. It is known that interface behavior is significantly influenced by factors that can be roughly classified into two categories. The first category includes particle-dependent, or micromechanical characteristics such as particle size and shape, relative particle displacement, relative particle rotation, and particle damage, such as fracture or grain crushing. The second category includes the influence of boundary conditions, roughness of the shearing surface, the stress level, and the deformation history. In this article we attempt to enhance our understanding of interfacial shear zone formation and behavior with emphasis on the effects of particle damage and grain crushing.

Due to the nature of particulate media, it is very difficult to experimentally measure anything other than macroscopic effects. For example, the interface region cannot be instrumented or probed without significantly influencing the behavior of the interface. Therefore, the amount of detailed laboratory information on micromechanical behavior in general, and behavior in interface regions in particular, is significantly limited. To aid in the study of interface behavior, many researchers have employed the discrete element method (DEM), which was pioneered by Cundall and Strack [1] for applications to granular media. While DEM has limitations on the number of particles that may be modeled, difficulty in accurately defining some material properties, and model calibration (which is probably the most significant limitation), it still has been able to provide valuable insight into interface behavior that otherwise would be unavailable. Jensen et al. [2] employed DEM with an enhancement, called *clustering,* to investigate the influence of micromechanical characteristics such as particle shape, particle rotations, and surface roughness on the behavior of soil-structure interfaces. In Jensen et al. [3], the use of several additional cluster configurations was demonstrated. In this paper, we present an investigation using DEM and clustering to numerically model particle damage, or grain crushing, and its influence on interface behavior.

A. DEM and clustering

Only a brief introduction to DEM and clustering will be given here. A more thorough discussion is given in earlier papers [2, 3]. DEM is a numerical technique where individual particles are represented as rigid bodies in either two- or three-dimensional space. In two dimensions each DEM particle has three degrees of freedom (two translations and one rotation), and in three dimensions each DEM particle has six degrees of freedom (three translations and three rotations). Each DEM particle can be in contact with neighboring DEM particles or structure boundaries. The contact between two DEM particles, or a DEM particle and a boundary, is modeled with a spring and dashpot in both the normal and tangential directions. The normal-direction spring has a no-tension constraint. In the tangential direction, if the tangential force reaches a Coulomb friction limit (given by the product of the compressive force and a user-specified coefficient of friction), it is allowed to slide. Small amounts of viscous damping are often included to help provide dissipation of high-frequency motion. The forces generated at a contact are computed based on the overlap of the bodies at the contact and the stiffness of the springs. Essentially, the method approximates compatibility where the interface spring stiffnesses serve as penalty numbers that approximately enforce impenetrability and presliding stick constraints. The forces from all of the contacts on a single body are summed yielding a resultant force, which is then used to compute the acceleration of the body according to Newton's law of motion. After the acceleration is determined, new velocity and displacement for the DEM particle is computed using central

difference explicit time integration. With the newly computed displacement configuration, the state of deformation at existing contacts is re-evaluated, and the possible creation of new contacts is evaluated, leading to a new cycle of computation.

Clustering is an enhancement to DEM. It is a simple means of modeling particles of complex shape. The basic idea is to combine several DEM particles of simple shape, such as discs or spheres, into one particle of more complex shape that we call a cluster. As shown in Figures 1(a) and (b), a simple circular DEM particle is not likely to give a good representation of the geometry of a natural particle such as a grain of sand. However, if an assemblage of simple DEM particles, such as discs, are used as shown in Figure 1(c), then a closer representation of a natural particle's geometry can be achieved. The only requirement is that the DEM particles that constitute a cluster must translate and rotate as essentially a rigid body. There are several possible ways to achieve this. In Jensen et al. [2, 3] and in this article, the intra-particle contacts within a cluster are constrained to be linear elastic in both the normal and tangential directions, thus allowing the normal-direction springs to support both compressive and tensile forces. Hence, the clusters we use here are semi-rigid. Implementation of clustering in DEM programs is straightforward. All DEM particles comprising a cluster retain separate degrees of freedom, and the program continues to use its existing contact detection algorithm, which for discs in two dimensions and spheres in three dimensions are very efficient. The only change is in the force computation for contacts between intra-cluster particles. This modification is elementary, and consists of assigning a "flag" to each contact. If the flag indicates the contact is conventional (i.e., a contact between two DEM particles that are not members of the same cluster), then the force computation proceeds unchanged, while if the flag indicates the contact is intra-cluster, then the force computation terminates after the liner-elastic predictor (i.e., it is simply linear elastic).

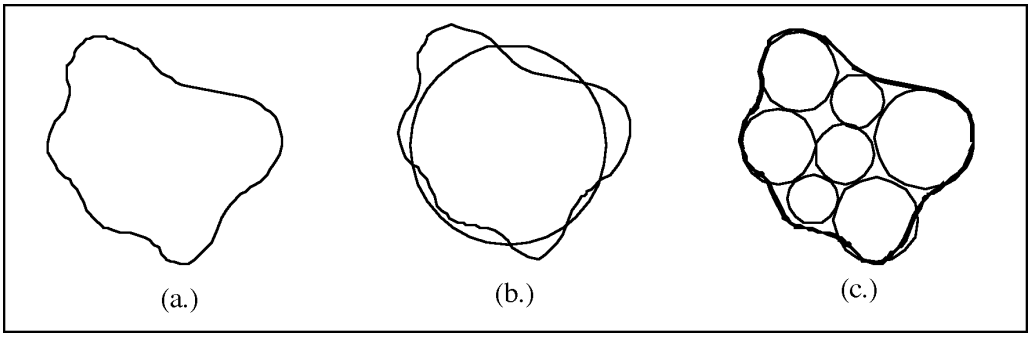

FIGURE 1 (a) Profile of sand particle. (b) Circular DEM element superimposed over a sand particle. (c) Assemblage of DEM particles joined together in a semi-rigid configuration, called a "cluster," which more closely resembles the geometry of an actual particle.

Another form of clustering has been reported in which displacement constraints are used to render a cluster to be truly rigid [4]. The benefit of such an approach is that the simple contact detection schemes for circular or spherical particles is retained, yet each cluster has only three or six degrees of freedom in two- and three-dimensions, respectively, regardless of the number of DEM particles that constitute the cluster. Compared to the scheme we use, rigid clustering is probably slightly more efficient in terms of computer time primarily because the internal force computation for intra-cluster contacts is not performed. While the substantial reduction of the number of degrees of freedom in rigid clustering may appear to render the explicit time integration loop much quicker, this phase of the solution is not time consuming, excepting the increased

number of internal force computations as described above. Furthermore, it does take additional time to impose and/or evaluate the displacement constraints which are repeatedly needed for the internal force computations and contact detections. For purposes of modeling damage, the major disadvantage of rigid clustering is that all intra-cluster force or stress measures are lost, or at best are only obtainable with difficulty. The method we use in this article automatically provides useful intra-cluster force and stress measures which potentially can be employed in damage criteria.

B. Grain crushing

Characterization of grain crushing has received fairly wide consideration. Mitchell [5] summarized the findings of Lee and Farhoomand [6] who determined that particle size, shape, soil gradation, and mineralogy factor into the degree of particle damage that occurs. These findings are (1) coarse granular soils have more particle breakage than fine soils, (2) angular particles undergo more grain crushing than smooth particles, (3) uniform soils crush more than well-graded soils, (4) for a deformation process at a given stress level, grain crushing continues indefinitely, but at a decreasing rate, (5) volume change is dependent upon the major vertical (principal) stress, and (6) the higher the stress ratio (σ_1/σ_3) the higher the degree of grain crushing (where σ_1 and σ_3 represent the largest and smallest principal stresses, respectively). Hardin [7], Fukumoto [8] and Hagerty et al. [9] studied the relationship of strength and stress-strain behavior of soils with the degree of particle crushing under different testing conditions. The relationship between grain crushing and sliding (plastic) work during interface shearing was demonstrated by Zeghal [10] using data generated by Hoteit [11]. This relationship was derived from the work consumed in interface shearing and the change in the grain size distribution in the material.

Related to grain crushing of soils is the work done in modeling of cemented granular materials. Plesha and Aifantis [12] modeled compression failure of a cemented aggregate material using polygon shaped DEM elements with edge-to-edge contacts having finite tensile and shear strength. Bazant et al. [13] modeled fracture of an aggregate composite material such as concrete by representing the bonds between the aggregates as axial truss members. Bruno and Nelson [14] used DEM to model the microstructural behavior of sedimentary rock by overlaying an additional layer of cementation on the circular disks that represent the grains. The cementation layer behaves linear elastic until a failure point is reached. Trent and Margolin [15] modeled a cemented granular material with DEM using elastic bonds between each two adjacent particles that have a certain minimum separation and where failure was modeled by inserting a Griffith crack within each bond.

Limited work has been done in modeling grain crushing of particulate materials. Richman and Chou [16] modeled homogeneous granular shear flows where grain size reductions were experienced due to particle collisions. It was assumed that the mass lost in the collisions had no effect on the flow. Using polygonal DEM elements, Issa and Nelson [17] modeled fracture of a granular material. The granular particles were assumed to be linear elastic but subject to a fracture limit based on a maximum tensile stress criteria and diametrical loading. Once the limit was reached, the particle fractured along a designated plane and became two particles. The effect of particle damage on wave propagation through a granular material was modeled by Sadd and Gao [18] using a maximum tensile stress criteria. No post fracture behavior was addressed but it was suggested that in order to handle post fracture shape, one particle could be divided into two or more particles. However, implementation is not a trivial matter. Previously, there have been no methods which model grain crushing and encompass all of the following desirable features:

1. Treatment of post fracture behavior with no loss of mass or loss of influence of fragments.
2. Can easily handle more than one damage or fracture criterion.
3. Does not require a uniformly sized or homogeneous material.

By utilizing the DEM cluster scheme we describe here for modeling granular materials, all three of these features can be conveniently satisfied.

II. Particle Damage Criteria and Declustering

Damage, in the form of grain crushing, has been experimentally shown to be a significant factor in the formation of an interface zone [11], although as described earlier, detailed information on the micromechanics of such damage is very difficult to measure or determine in a laboratory specimen. One of the most significant features of clustering is the ability and ease with which damage can be modeled. The ability to numerically simulate damage phenomena can provide a great wealth of detailed micromechanical information that can greatly aid the understanding of interface behavior. To implement damage within DEM, we choose one or more criteria that specify when one or more individual DEM particles of a cluster disassociate, and we call this process *declustering.* When one of these criteria is met for a DEM particle in a cluster, the cluster is broken (partially or fully) by changing the links in the computer program that identify the DEM particle as being a member of a particular cluster. Since all of the DEM particles are recognized by the program as separate entities having independent degrees of freedom, the DEM particles that at one time comprise a cluster at some subsequent time may model the fragments of a cluster.

There appears to be two fundamental mechanisms by which particles can experience damage. The first is abrasion, or wear, such as occurs when one particle frictionally slides past another and is gradually abraded in the process. The second is damage due to overstressing in which a crack propagates through a particle, breaking it into two or more smaller particles. Because shear zone behavior is always accompanied by considerable localized frictional sliding, in this article we emphasize abrasion damage. Alternatively, damage due to fracture may be more appropriate for modeling a comminution process or a problem involving large compression loading and small relative displacements such as occur in wave propagation problems. Similar to Sadd and Gao [18] a damage criteria could be implemented wherein a maximum allowable normal force and/or shear force, or some function of these, would determine when damage due to overstressing occurs. Following Trent and Margolin [15] a damage criteria based on fracture mechanics could be developed.

A useful measure of the energy dissipated during frictional sliding of one particle against another is the sliding work (or plastic work), W. Because frictional forces always oppose the direction of relative sliding, the sliding work is nonnegative and is a nondecreasing function of time. We use an energy density criterion to decide if enough work has been accumulated by a particular DEM particle of a cluster to warrant its separation (breakage) from the cluster. This requires a user-specified critical energy density, W_0. For a particle i of a cluster, the product of W_0 with the DEM particle's volume V_i gives the sliding energy that the particle can absorb, $W_i^{\max}$, before breakage occurs

$$W_i^{\max} = W_0 V_i \tag{1}$$

Such a criterion allows particles of different sizes to be used in a model of a medium. The greater the value of W_0, the more resistant particles are to damage due to abrasion. Furthermore, a larger DEM particle in a cluster requires more work, or energy, for breakage to occur, than for a smaller DEM particle.

During the course of computation, the increment of sliding work done on a particular DEM particle i is easily computed at each time step by summing the work increments for all *extra-cluster*

contacts for the particle

$$dW_i = \sum_{\substack{\text{number} \\ \text{extra-cluster} \\ \text{contacts}}} f_t d\delta_t^S \tag{2}$$

where f_t is the tangential force at the contact, $d\delta_t^S$ is the increment of relative tangential plastic (sliding) displacement between the DEM particle and a contacting neighbor, and the summation excludes all intra-cluster contacts. The total work is obtained by integrating (summing) the work increments

$$W_i = \int dW_i \tag{3}$$

As long as $W_i < W_i^{\max}$ the cluster remains intact. If $W_{\geq} W_i^{\max}$ then the DEM particle separates from the cluster. The exact manner in which this separation occurs, and potential impact on other DEM particles within the cluster, depends on the geometry of the cluster, position of the separating DEM particle within the cluster, and previous particle separations for the cluster.

To develop scenarios for DEM particle separations from a cluster, we begin by requiring every particle within a cluster to have at least two intra-cluster contacts. Hence, the simplest cluster in our scheme consists of three DEM particles, as shown by cluster C3 in Figure 2. The merit of this requirement is that a semi-rigid arrangement of DEM particles can always be

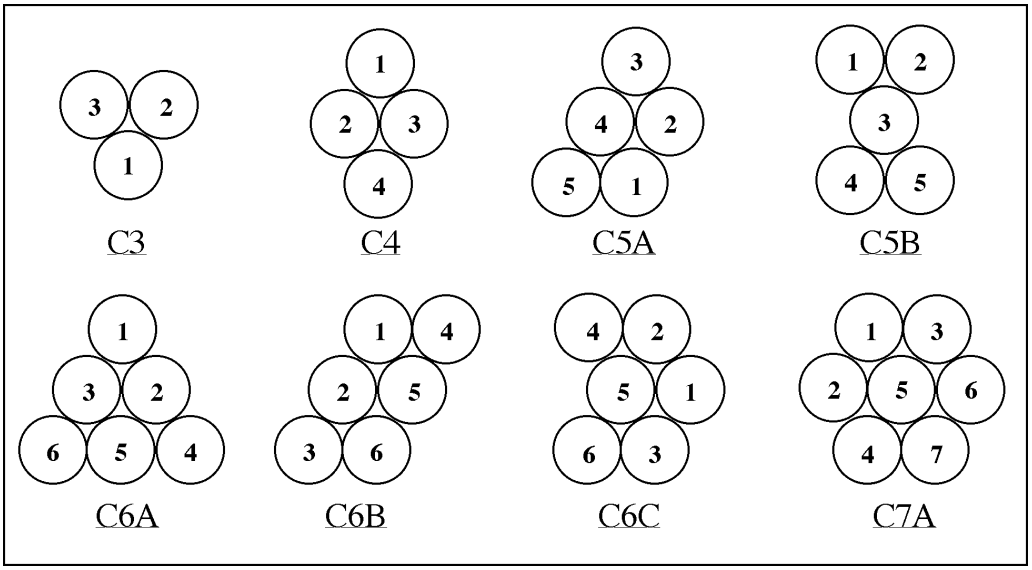

FIGURE 2 Definition of cluster geometries.

constructed using only normal and tangential contact springs. It is possible to develop a clustering scheme in which each DEM particle can have a minimum of only one intra-cluster contact, but to render such a cluster semi-rigid requires that a rotational contact spring be included at each contact along with the normal and tangential springs. While such an addition is fundamentally straightforward, the disadvantage is that implementation in DEM software requires far more extensive code revisions than anything discussed in this article. As clusters degrade, we require

each DEM particle remaining in the cluster to also maintain at least two intra-cluster contacts, for the same reasons as discussed above. For example, in the three particle cluster C3 shown in Figure 2, when the first DEM particle separates, the remaining two particles would each have only one intra-cluster contact and hence would not be semi-rigid. Under these circumstances we allow these DEM particles to also immediately separate in which case the cluster is fully destroyed leaving three DEM particles, each with independent motion. For clusters comprised of more than three DEM particles, there are several different scenarios in which individual particles can break off and each of these scenarios must be anticipated and accounted for. Figure 2 shows several different cluster types that we have implemented, and a local particle numbering system for each cluster. Table 1 lists the schemes and order in which the DEM particles could break off of a cluster. The table is to be used in conjunction with Figure 2 and is read as follows. The first column identifies the cluster type. The second column identifies the local number of the DEM particle that is breaking off the cluster. The next set of columns, entitled "Declustering Scheme," details the possible cluster configurations that remain after a particular particle has broken off. For example, if particle number 1 of a C6A cluster were to break off, the result would be one C5A cluster and one single particle. The C5A cluster that remains now obeys the declustering scenarios listed in that column of Table 1 where we note that its constituent DEM particles will likely have accumulated some sliding energy from earlier deformations.

III. Breakage Factor as a Measure of Damage

A quantitative measure of the extent of damage in a particulate material is useful, and to this end we will employ the *breakage factor*, which compares the initial median particle size to the final median particle size. Soils are graded according to how well-distributed the soil particle sizes are based upon the portions of a medium's mass or weight that are retained in a series of sieves. Zeghal [10] determined that a very suitable measure for the breakage factor B is the ratio

$$B = \frac{D_{50i}}{D_{50f}} \tag{4}$$

where D_{50} is defined as the grain size for which 50% of the soil by weight is smaller and the subscripts i and f refer to *initial* and *final*, i.e., before and after the shear event. For application to DEM models with clusters, D_{50} is computed as follows:

$$D_{50} = \frac{\sum m_i D_i}{\sum m_i} \tag{5}$$

where the summation ranges over the number of clusters plus the number of individual DEM particles that are not members of a cluster, i denotes the cluster or DEM particle number, m_i and D_i are the mass and minimum diameter of cluster i or particle i, respectively.

Selection of a value for the critical energy density W_0 of Equation 1 is important as it controls the rate at which abrasion damage occurs in our damage scheme. In order to determine a value that would correspond to a natural material, several trial DEM simulations of laboratory shear tests were conducted using different values of the critical energy density. The DEM simulations used C3, C4, C5A or the combination of different cluster types described as CMIX in Section IV. A typical DEM discretization is shown in Figure 3, and additional details of the computations are given in Section IV. For each value of critical energy density used, the breakage factor was computed and plotted versus the sliding work per unit area done on the DEM particle mass, where the area was taken to be the product of the domain length (15 mm) and thickness (1 mm). These plots were then compared to the breakage factor versus sliding work per unit area plots prepared by Zeghal [10] from experimental work done by Hoteit [11]. In Hoteit's work, the amount of grain

TABLE 1

Declustering Schemes for Modeling Particle Damage with Clusters

Cluster Type	Particle Breaking off	Declustering Scheme					
		Single	C3	C4	C5A	C5B	C6C
C3	1 or 2 or 3	3					
C4	1 or 4	1	1				
	2 or 3	4					
C5A	1 or 2	2	1				
	3 or 5	1		1			
	4	5					
C5B	1 or 2 or 4 or 5	2	1				
	3	5					
C6A	1 or 4 or 6	1			1		
	2 or 3 or 5	3	1				
C6B	1 or 6	2		1			
	3 or 4	1			1		
	2 or 5	3	1				
C6C	4 or 6	1			1		
	2 or 3	2		1			
	1	1				1	
	5	6					
C7A	1 or 2 or 3 or 4 or 6 or 7	1					1
	5	7					

crushing in a thin layer of material containing a shear zone was determined for tests on uniformly graded quartz sand (three different size groups were used) and well-graded calcareous sand (one size) with consideration of the effects of initially loose and initially dense states, and constant compressive stress and constant volume boundary conditions. The value of critical energy density that gave the best correlation was found to be 10^7 J/m^3, and the resulting agreement between the numerical simulations and the results of Hoteit's experiments is shown in Figure 4. While there is some scatter in the data of Figure 4, it is remarkable that the breakage factor for initially loose and initially dense media, and constant stress and constant volume boundary condition tests appears to be uniquely related to sliding work. Because of a lack of data for other types of sand, it is not known how universally applicable this value of critical energy density is. Full elucidation of this awaits additional laboratory and computational testing.

IV. Simulations Using Declustering

Numerical experiments were conducted to demonstrate the utility of declustering for modeling particle damage, and to study the effects of particle damage on structure-media interfaces. These simulations were performed in two-dimensions, and a typical discretization is shown in Figure 3. The domain consists of a rough horizontal structure surface at the bottom, a horizontal boundary at the top, and two vertical periodic boundaries. The medium shown in this example consists of 500 clusters of various size and shape as described below. The clusters are generated with initially random position, and are then consolidated by applying a compressive force to the upper horizontal boundary. The width of the domain is 15.0 mm and the approximate height after consolidation is also 15 mm. Once the consolidation is complete, the upper boundary is subjected

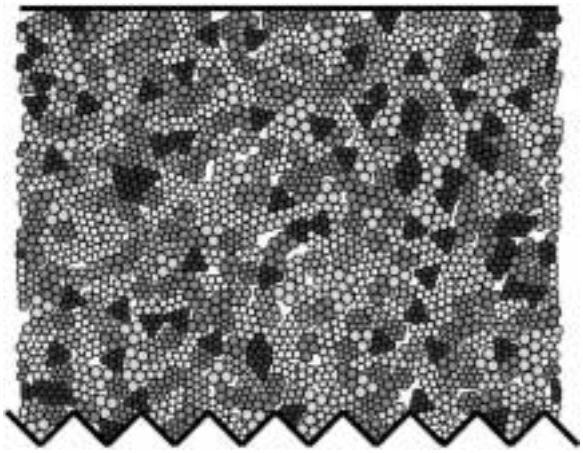

FIGURE 3 Typical DEM model of a granular material. This particular model employs 500 clusters of various shape. Vertical boundaries at left and right are periodic boundaries.

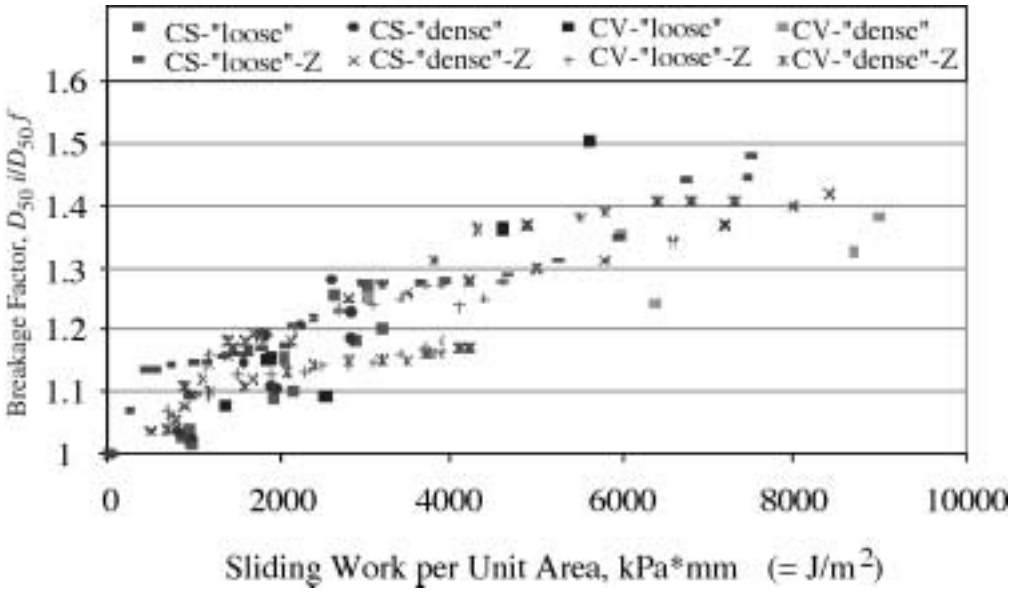

FIGURE 4 Plot of breakage factor vs. sliding work per unit area. The breakage factor is a measure of the degree of damage the particles have undergone. Data is from both constant stress and constant volume tests (denoted in the legend by "CS" and "CV," respectively), and initially "loose" and "dense" media. The DEM models used C3, C4, C5A or CMIX (as described in Section IV) clusters. Data from numerical simulations were obtained using a critical energy density of $W_0 = 10^7$ J/m^3 and are plotted as solid points. The data from Zeghal [10], based on laboratory tests, are plotted as the wire points and are designated by **Z** in the legend.

to either a prescribed compressive load (for a constant normal stress test), or a prescribed constant displacement (for a constant volume test). For the constant normal stress tests, the upper horizontal boundary was subjected to a normal force of 33.3 N which corresponds to a 35 kPa normal stress. As described in Jensen, et al. [2], the periodic boundaries allow DEM particles that pass out of one boundary to be automatically reintroduced at the opposite boundary, thus effectively modeling a domain with infinite horizontal extent. Because of the periodic boundaries, the domain

TABLE 2

Size of the Individual DEM Particles that Comprise Clusters

Cluster Type	Individual DEM Particle Diameter, mm
Single	0.300
C3	0.173
C4	0.150
C5A	0.134
C6A	0.122
C6B	0.122
C6C	0.122
C7	0.113

can be viewed as representing a two-dimensional vertical section of a conventional ring shear device. Computations were performed to investigate the effects of larger domain height, and larger domain width for constant stress simulations with and without damage with the conclusion that no significant changes in results were produced. The coefficient of friction for contact between two DEM particles or a DEM particle and a surface is 0.4, similar to the coefficient of friction for quartz particle-quartz particle contact [19]. The normal and shear stiffnesses for particle-particle and particle-structure contacts are 1.2×10^6 N/m. These stiffnesses were computed using Hertz theory for contact between two spherical bodies [20] with the modulus of elasticity for quartz. For the simulations that include damage, the critical energy density is taken as $W_0 = 10^7$ J/m^3. The shearing surface (i.e., structure surface) has sawtooth-shaped roughness with $\pm 45^\circ$ angles of inclination with respect to the horizontal. The period of the surface roughness (distance from the top of one sawtooth to the top of the next sawtooth) is $3D$ where D is the diameter of a single, individual DEM particle. To represent far-field effects, the DEM particles in contact with the upper horizontal surface are “glued” to that surface by restricting them to have no rotation, no horizontal displacement, and the same vertical displacement as the boundary. Such treatment is used to help insure that if a shear zone forms, it will not be immediately along this boundary. For all analysis cases, the rough structure surface was given a uniform slow shear velocity up to a total shear displacement of 6.3 mm.

The simulations include an initially “loose” medium and an initially "dense" medium for models using each of the following cluster types: non-clustered DEM particles (Single), three particle clusters (C3), five particle clusters (C5A), and mixed cluster types (CMIX). The non-clustered models have 500 single DEM particles. Each of the clustered models contains 500 clusters except in the case of the mixed models which contain 500 clusters as follows: 50 three particle clusters, and 75 clusters each of the C4 four particle clusters, C5A five particle clusters , the C6A six particle cluster, the C6B six particle cluster, the C6C six particle cluster, and the C7A seven particle cluster. Table 2 gives the diameter of a single DEM particle and the diameters of the DEM particles that make up each cluster. The “loose” medium models were created using the consolidation procedure described above. By taking the loose medium models, and temporarily setting the interparticle coefficient of friction to zero, additional consolidation is achieved leading to the “dense” medium models. After the dense medium models were fully compacted, the interparticle coefficient of friction was then set back to 0.4 for the subsequent simulation.

The results will be discussed in the following order. First, the constant stress simulations with no particle damage (no declustering) will be compared to the corresponding constant stress

simulations which have damage (declustering). Then, the constant volume simulations with no damage will be discussed with respect to the constant volume simulations with damage. Next, the constant stress simulations without damage will be measured against the constant volume simulations without damage. Lastly, the constant stress simulations with damage will be compared to the constant volume simulations with damage. The results of these numerical analyses are summarized in four figures. These figures are montages of graphs containing shear force versus tangential displacement, normal displacement versus tangential displacement, average displacement of DEM particles within a horizontal layer versus the vertical position of the horizontal layer, and the average rotation of the DEM particles within a horizontal layer versus the vertical position of the layer. Each domain was divided into ten horizontal layers of equal depth. The average DEM particle displacement within a horizontal layer is taken to be the mean displacement of all particles within the layer. Similarly, the average rotation of the DEM particles in a horizontal layer is taken as the mean rotation of the particles within the layer. Figure 5 is the montage of "loose"

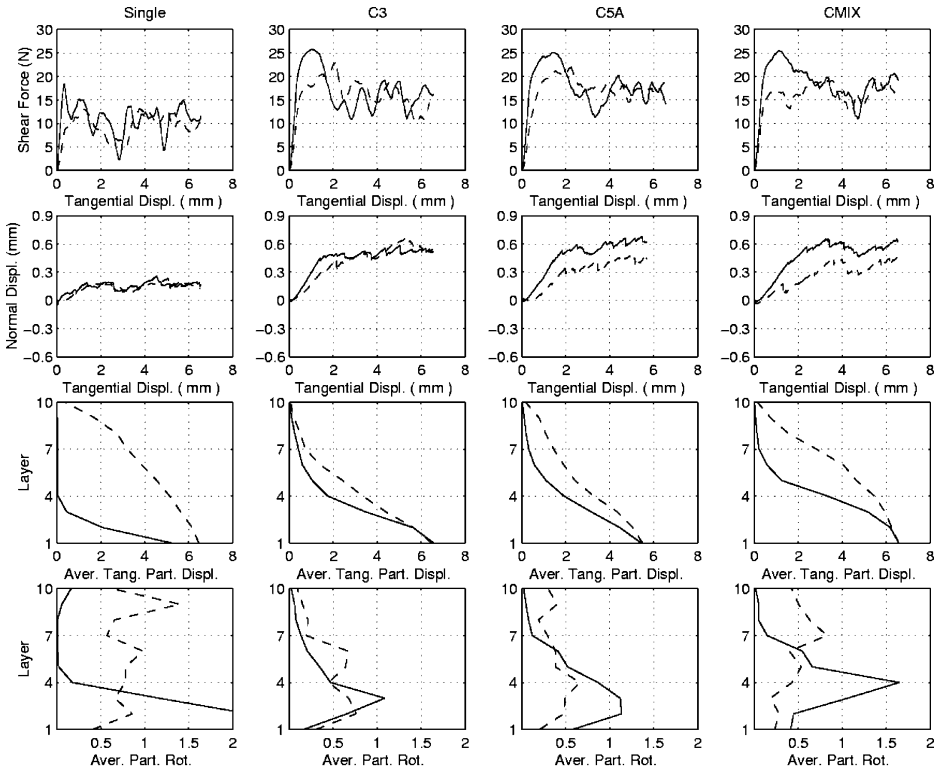

FIGURE 5 Constant compressive stress DEM simulations. Graphs of shear force at shearing surface vs. tangential displacement of shearing surface, dilation of top surface vs. tangential displacement of shearing surface, horizontal layer vs. average displacement of DEM particles in layer, and horizontal layer vs. average rotation of DEM particles in layer for the data sets with single particles, three particle clusters (C3), five particle clusters (C5A), and a set of mixed clusters (CMIX). Dashed lines represent the initially loose media and the solid lines represent the initially dense media. These simulations do not include particle damage.

and "dense" data sets under constant stress boundary conditions without damage (declustering). Figure 6 is the montage of "loose" and "dense" sets under constant stress boundary conditions but with damage. Figure 7 is the montage of "loose" and "dense" data sets under constant volume

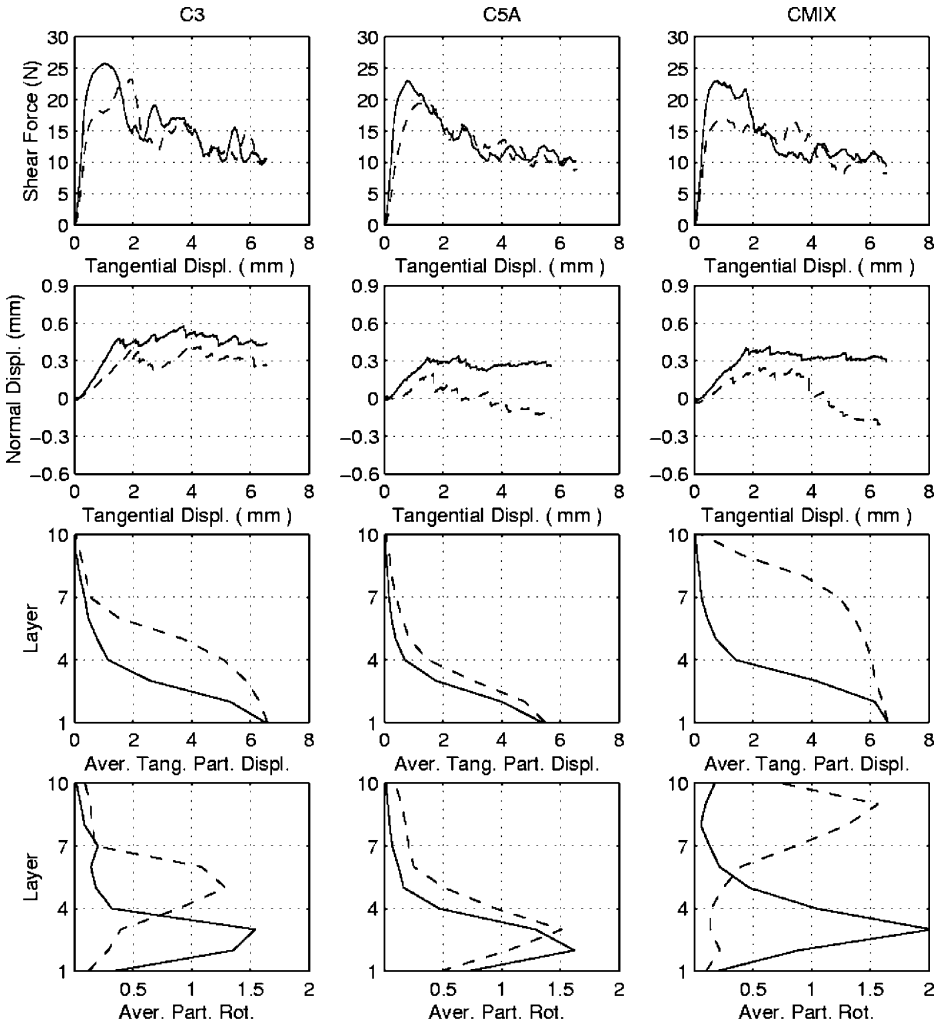

FIGURE 6 Constant compressive stress DEM simulations. Graphs of shear force at shearing surface vs. tangential displacement of shearing surface, dilation of top surface vs. tangential displacement of shearing surface, horizontal layer vs. average displacement of DEM particles in layer, and horizontal layer vs. average rotation of DEM particles in layer for the data sets with three particle clusters (C3), five particle clusters (C5A), and a set of mixed clusters (CMIX). Dashed lines represent the initially loose media and the solid lines represent the initially dense media. These simulations include particle damage.

boundary conditions with no damage. Figure 8 is the montage of “loose” and “dense” sets under constant volume boundary conditions but with damage. In Figures 5 through 8, the “loose” data sets are represented by the dashed lines, while the “dense” data sets are represented by the solid lines.

A. Effects of Damage - “Loose” and “Dense” Media Under Constant Stress Conditions

These simulations are performed under uniform compressive load boundary conditions. Comparison of the shear force versus tangential displacement plots of Figures 5 and 6 show

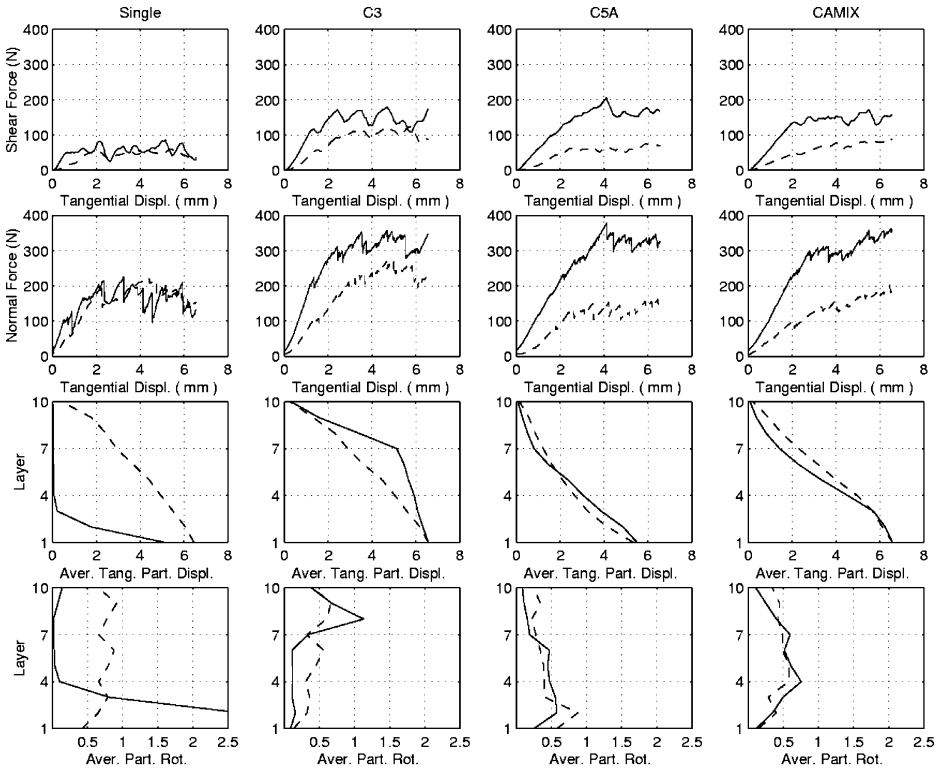

FIGURE 7 Constant volume DEM simulations. Graphs of shear force at shearing surface vs. tangential displacement of shearing surface, normal force at shearing surface vs. tangential displacement of shearing surface, horizontal layer vs. average displacement of DEM particles in layer, and horizontal layer vs. average rotation of DEM particles in layer for the data sets with single particles, three particle clusters (C3), five particle clusters (C5A), and a set of mixed clusters (CMIX). Dashed lines represent the initially loose media and the solid lines represent the initially dense media. These simulations do not include particle damage.

there is a small decrease in peak shear stress in the data sets with damage. The magnitude of the steady state shear stress is also lower in the sets with damage. When comparing the plots of average tangential (horizontal) particle displacement in a horizontal layer versus the layer position, shown in Figures 5 and 6, it is seen that there is a pronounced shear zone that forms when damage is included, and with no damage a distinct shear zone is not evident. In agreement with this observation are the plots of average DEM particle rotation in a horizontal layer versus the layer position, shown in Figures 5 and 6, where formation of a distinct process zone occurs in the same locations as indicated above when damage is included, and when there is no damage there is no such evidence. We have found that presence of localized pronounced DEM particle rotations is frequently a good indicator of shear zone formation. In fact, the presence of large particle rotations will sometimes indicate some type of process zone when the average particle displacements do not reveal such a zone. The plots of normal displacement of the upper horizontal boundary versus tangential displacement of the shearing surface, shown in Figures 5 and 6 indicate that simulations with damage exhibit less dilation with two of the sets, C5A “loose” and CMIX “loose,” and comparable dilation with the remaining sets. The compression occurs as a result of declustering and the smaller cluster fragments being able to more efficiently fill available void space.

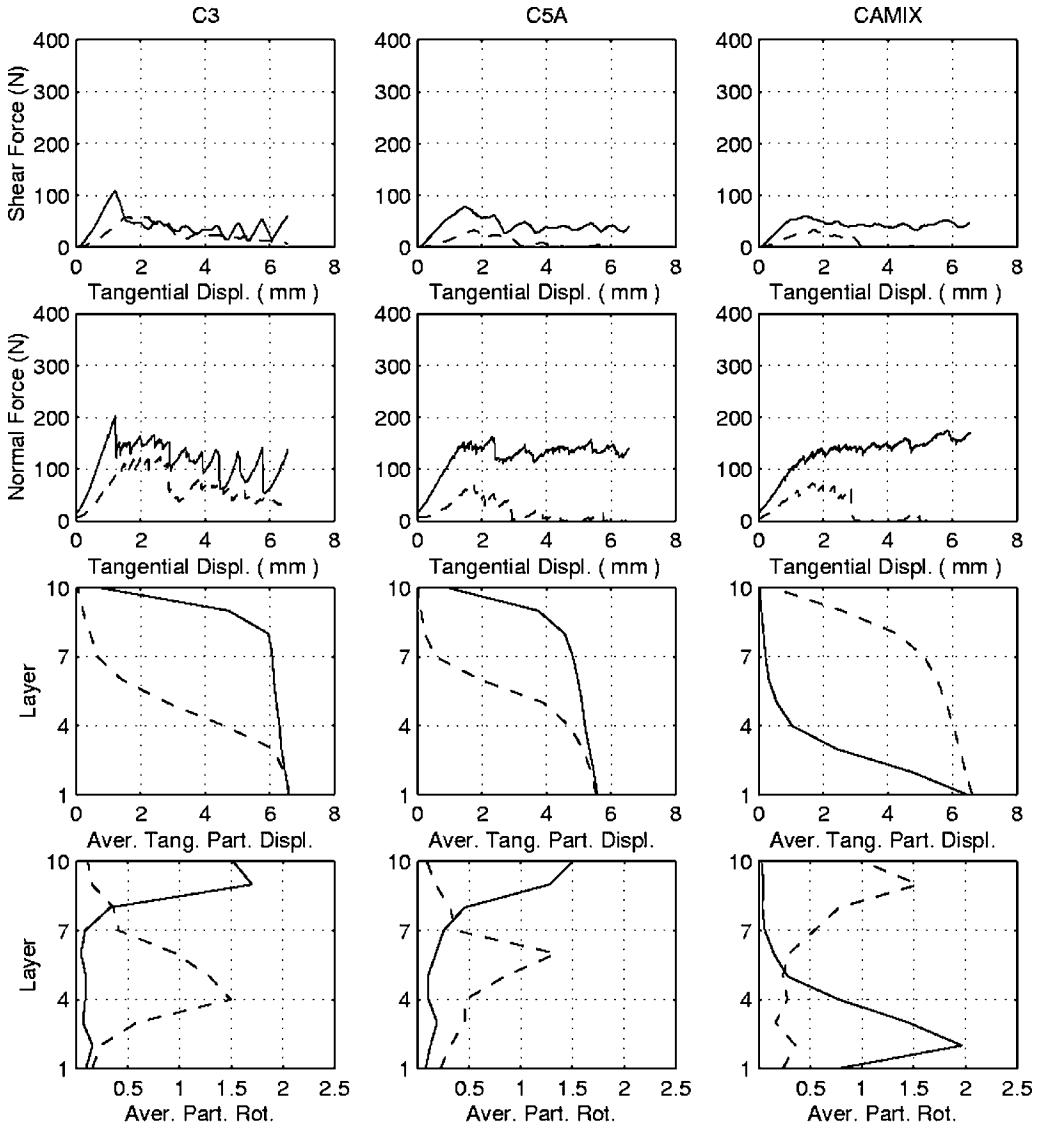

FIGURE 8 Constant volume DEM simulations. Graphs of shear force at shearing surface vs. tangential displacement of shearing surface, normal force at shearing surface vs. tangential displacement of shearing surface, horizontal layer vs. average displacement of DEM particles in layer, and horizontal layer vs. average rotation of DEM particles in layer for the data sets with three particle clusters (C3), five particle clusters (C5A), and a set of mixed clusters (CMIX). Dashed lines represent the initially loose media and the solid lines represent the initially dense media. These simulations include particle damage.

B. Effects of Damage - “Loose” and “Dense” Media Under Constant Volume Conditions

These simulations are performed under constant volume boundary conditions. That is, after the initial consolidation of the medium, the upper horizontal surface of the model is constrained to have no motion thus proving a domain that has constant volume and hence, no net dilation. In all

cases, both the normal and shear forces increase dramatically with increasing shear displacement. As can be seen in the shear force and normal force versus tangential displacement plots of Figures 7 and 8, as the rough structure surface is sheared, the forces increase dramatically, by as much as one order of magnitude when there is no damage, when compared with the corresponding plots of Figures 5 and 6. These force increases, of course, arise because the medium is constrained to have zero average dilation (no volume change). Since relative sliding of one particle past another, which must occur for the medium to undergo the shear displacement that is prescribed, requires locally dilatant deformations, the remainder of the medium must compress to accommodate this. Because of the stiff nature of DEM particles, especially when clusters are not allowed to damage, very large normal forces are produced, which in turn require correspondingly large shear forces.

In actual laboratory tests with natural media, such behavior is also present. Constant volume laboratory tests reported by Sengara [21] show an increase in shear forces up to a factor of about two compared to constant stress tests, while tests reported by Hoteit [11] show increase up to a factor of about five. Thus, the constant volume DEM simulations with no damage substantially over predict the shear force behavior of natural media. The DEM simulations with damage, shown in Figure 8, are substantially improved and display increases of factors of about three to four compared to the simulations shown in Figure 6, and are in reasonable agreement with natural media. The improved results for DEM with damage is due in part to the creation of cluster fragments that can more easily rearrange and occupy available void space, and hence allow the DEM medium to better accommodate the shear deformation. As can be seen in the average DEM particle displacement versus horizontal layer position plots of Figures 7 and 8, a shear zone is more pronounced when there is damage than in the simulations without damage. As also shown in Figures 7 and 8, the location of the peak average DEM particle rotations also correspond to the locations of shear zone formation.

While the agreement between DEM simulations with damage and natural media is encouraging, it should be noted that there are some possible fundamental differences between DEM media and natural media that are not yet understood and accounted for. First is that DEM media are inherently stiff. While the abrasion damage discussed in this article is a softening mechanism, there may also be other forms of damage present in natural material, such as particle fracturing due to overstressing. Also, the DEM particles used here are two-dimensional whereas natural particles are three-dimensional and undergo three-dimensional motion even when the macroscopic medium motion is nominally two-dimensional.

C. Effects of Constant Stress vs. Constant Volume BCs - No Particle Damage

These comparisons are made from Figures 5 and 7. The most obvious comparison between the constant stress and constant volume simulations is that the peak shear and normal forces of the constant volume tests are nearly one order of magnitude greater than those of the constant stress tests, and possible reasons for this were previously discussed. However, the peak average DEM particle rotations in the constant volume simulations are comparable to those in the constant stress simulations in both magnitude as well as location. This suggests that particle rotations are not functions of stress level, but are dependent upon particle shape and particle displacement. As can be seen in Figures 5 and 7, the plots of average DEM particle displacement in a horizontal layer versus position of the layer for the “loose” medium models, for both the constant stress tests and the constant volume tests, have the same basic shape and show a poorly defined shear zone. This is in contrast to the plots of average DEM particle displacement in a horizontal layer versus position of the layer for the “dense” medium models, where both the constant stress and the constant volume results also have the same shape but with much more distinct shear zones.

D. Effects of Constant Stress vs. Constant Volume BCs - Including Particle Damage

These comparisons are drawn from Figures 6 and 8. Again, as can be seen in the plots of normal force and shear force versus tangential displacement, the peak forces are much greater in the constant volume tests than in the constant stress tests. Since the clusters are allowed to accumulate damage, enough of the clusters are broken in the "loose" constant volume test that the particles reconsolidate to a volume less than the initial volume of the medium and thus the normal and shear forces eventually go to zero. As can be observed from the plots of average DEM particle rotation in a horizontal layer versus position of the layer, shown in Figures 6 and 8, we see good agreement between the values and distributions of particle rotations for the constant stress simulations and the constant volume simulations. All of the simulations developed very pronounced shear zones, although occasionally the location of a shear zone changes from being close to the structural surface to being closer to the upper horizontal boundary of the domain. This is subsequently discussed in greater detail.

E. Remarks

Some general observations on the behavior of particulate media can be made:

1. Constant volume tests result in peak normal and shear forces that are much higher than those found in constant stress tests.
2. Particle damage appears to play a strong role in the formation of shear zones. The location of shear zones found in constant stress tests and in constant volume tests is very similar.
3. The location of the peak average particle rotation and the distribution of particle rotations correspond to the location of shear zone formation as determined by the particle displacement distribution. Also, the peak average particle rotations for the constant stress tests were generally comparable to those for the corresponding constant volume tests.
4. The shear zones found in the tests that include damage were always significantly more pronounced than those found when damage was not considered. When damage was not considered, a definite shear zone was usually not present.
5. Particle damage results in a small reduction in the peak and steady state normal and shear forces for the constant stress tests, and a large reduction in the peak and steady state forces for the constant volume tests. Damage also reduced the amount of dilation in the constant stress tests. Of particular note is the use of damage (declustering) substantially improves the accuracy of DEM for modeling constant volume situations.

In addition to the foregoing remarks, some observations on the relationship between damage of DEM clusters and natural media can be made. As previously reviewed, Mitchell [5] has summarized the factors that contribute to the degree of particle damage that occurs. How declustering relates to two of these will be discussed. First, angular particles undergo more grain crushing than smooth particles. Figure 9 shows a plot of breakage factor versus sliding work per unit area for both initially "loose" and "dense" DEM media of the C3, C4, and C5A cluster types. The *angularities*, based on Lee's [22] method, are 513, 532, and 702, for the C3, C4, and C5A cluster types, respectively [3]. The larger this measure, the greater is the particle angularity. Therefore, the C5A cluster type is the most angular of the three cluster types considered. As can be seen in

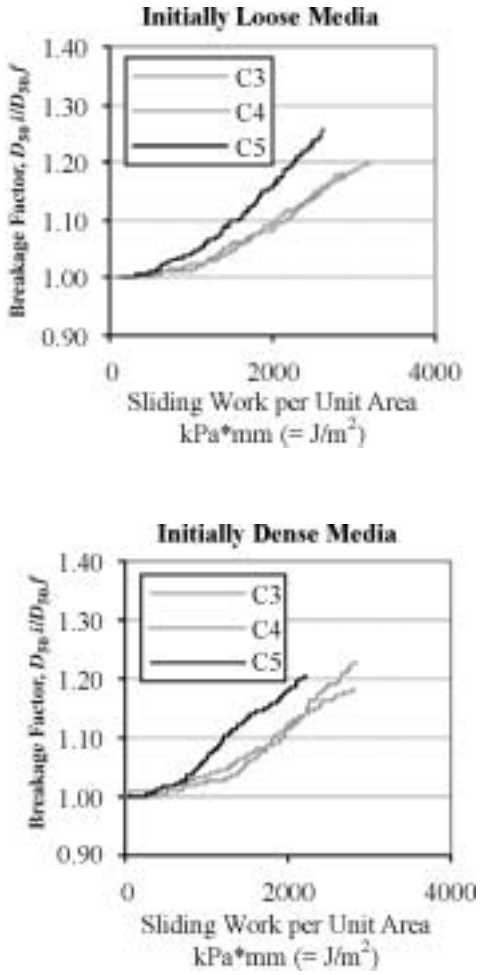

FIGURE 9 Graphs of breakage factor vs. sliding work per unit area for initially "loose" and "dense" DEM media with C3, C4, and C5A cluster types. C5A clusters are more angular than either C3 or C4 clusters. These graphs show that more breakage occurs at the same magnitude of sliding work for the more angular cluster types.

Figure 9, for a given value of sliding work, the breakage factor of the C5A cluster type is greater than that of either the C3 and C4 cluster types. Since the breakage factor is directly proportional to particle damage, declustering seems to realistically model this aspect of particle damage.

A second observation is that during a deformation process, particle damage continues to evolve indefinitely, although at a decreasing rate. This effect is best seen in Figure 10 which is a plot of the breakage factor versus sliding work per unit area for the initially "dense" media simulations with both constant stress as well as constant volume boundary conditions. The thin data lines are the constant volume data sets and the thick lines are the constant stress data sets. As more work is done on the system, fewer DEM particles tend to break. The constant volume simulations show this better since more total work is done due to the very large forces that arise.

While our simulations usually show that shear zones develop close to the structural surface, occasionally the shear zone develops closer to the upper horizontal boundary of the domain; see for example the average tangential particle displacement vs. layer number for the initially dense

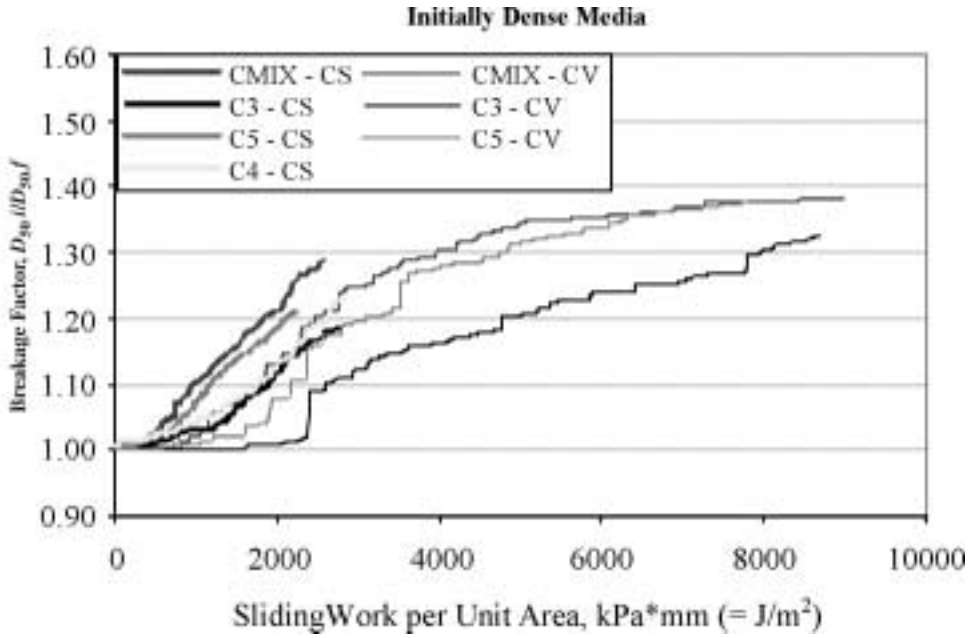

FIGURE 10 Graph of breakage factor vs. sliding work per unit area for initially "dense" DEM media. Graph shows a diminishing number of DEM particles breaking as sliding work increases.

C3 simulation in Figure 7. It appears that while there is preference for shear zones to form near structural surfaces, this preference is not strong and due to effects such as local packing of particles, etc., conditions may occasionally be more favorable for the shear zone to form elsewhere in the medium. In connection with this, we note the results of Jensen et al. [3] (Figure 7) where it is shown that structural surface roughness does not affect the interface friction angle, provided the structural surface is sufficiently rough to engage a thin layer of particles, which then move with the structural surface. Under these conditions, there would seem to be little difference between conditions near the structure surface, as opposed to other locations in the medium.

V. Conclusions

An enhancement to the discrete element method that effectively models particle damage in particulate media-structure interfaces has been presented. The enhancement is based on clustering whereby particles of complex shape are modeled by combining several DEM particles of simple shapes into a semi-rigid assemblage. The individual DEM particles that constitute a cluster are allowed to decluster, or break off according to a sliding energy criteria and thereby model grain crushing. Numerical "experiments" simulating ring shear tests were performed to demonstrate the importance of damage and the effectiveness of declustering for modeling grain crushing. The numerical experiments were conducted using varying boundary conditions, cluster types and initial medium densities. Both constant volume tests and constant stress tests were performed. In constant volume tests, peak shear and normal stresses were dramatically reduced when damage (declustering) was implemented, thus substantially improving DEM's ability to model such boundary conditions. More distinct shear zones were noted in the results of both the constant volume and the constant stress tests when damage was included. This was done without significant loss of shear strength of the particle mass. The degree of particle crushing, as measured by the breakage factor, was also compared to experimental results. The amount of damage for

a value of critical energy density equal to 10^7 J/m^3 corresponded very well with experimental values. Damage and declustering also demonstrated good agreement with two factors that are commonly accepted as having a strong impact on the extent of particle damage in a medium. These include a demonstration that angular particles display a greater rate of damage than less angular particles, and that during a deformation process damage continues to accumulate but at increasing slower rates.

References

[1] **Cundall, P.A. and Strack, O.D.L.,** A discrete numerical model for granular assemblies, *Geotechnique,* **29**, 47–65, 1979.

[2] **Jensen, R.P., Bosscher, P.J., Plesha, M.E., and Edil, T.B.,** DEM simulation of granular media-structure interface: effects of surface roughness and particle shape, *Int. J. Numer. Anal., Methods Geomech.,* **23**, 531–547, 1999.

[3] **Jensen, R.P., Edil, T.B., Bosscher, P.J., Plesha, M.E., and Ben Kahla, N.** Effects of particle shape on interface behavior of DEM-simulated granular materials, *Int. J. Geomechanics*, to appear, 2001.

[4] **Thomas, P.A. and Bray, J.D.,** Capturing nonspherical shape of granular material with disk clusters, *J. Geotech. Eng.,* **125**, 169–178, March, 1999.

[5] **Mitchell, J.K.,** *Fundamentals of Soil Behavior,* 2nd edition, Wiley, New York, 1993.

[6] **Lee, K.L. and Farhoomand, I.,** Compressibility and crushing of granular soil in anisotropic triaxial compression, *Can. Geotech. J.,* **4**, 68–86, 1967.

[7] **Hardin, B.O.,** Crushing of soil particles, *J. Geotech. Eng.,* **111**, 1177–1192, March, 1985.

[8] **Fukumoto, T.,** Particle breakage characteristics of granular soils, *Soils Found.,* **32**, 26–40, 1992.

[9] **Hagerty, M.M., Hite, D.R., Ullrich, C.R., and Hagerty, D.J.,** One-dimensional high-pressure compression of granular media, *J. Geotech. Eng.,* **119**, 1–18, March, 1993.

[10] **Zeghal, M.,** *Modeling of Sand-Structure Interfaces,* Ph.D. thesis, University of Wisconsin-Madison, Department of Civil and Environmental Engineering, 1993.

[11] **Hoteit, N.,** *Contribution a l'Etude du Comportment d'Interface Sable Inclusion at Application au Frottement Apparent,* Doctorate Thesis, Institut National Polytechnique de Grenoble, France, 1990.

[12] **Plesha, M.E. and Aifantis, E.C.,** On the Modeling of Rocks with Microstructures, Proceedings of the 24th U.S. Rock Mechanics Symposium, C.C. Mathewson, editor, 27–35, 1983.

[13] **Bazant, Z.P., Tabbara, M.R., Kazemi, M.T., and Pijaudier-Cabot, G.,** Random particle model for fracture of aggregate or fiber composites, *J. Eng. Mech.,* **116**, 1686–1705, 1990.

[14] **Bruno, M.S., and Nelson, R.B.,** Microstructural analysis of the inelastic behavior of sedimentary rock, *Mech. Mater.,* **12**, 95–118, 1991.

[15] **Trent, B.C. and Margolin, L.G.,** A numerical laboratory for granular solids, *Eng. Comput.,* **9**, 191–197, 1992.

[16] **Richman, M.W. and Chou, C.S.,** A Theory for Grain-Size Reduction in Granular Flows of Spheres, *Z. Angew. Math. Phys.,* **40**, 883–898, 1989.

[17] **Issa, J.A. and Nelson, R.B.,** Numerical Analysis of Micromechanical Behaviour of Granular Materials, *Eng. Comput.,* **9**, 211–223, 1992.

[18] **Sadd, M.H. and Gao, J.Y.,** The Effect of Particle Damage on Wave Propagation in Granular Materials, *Mechanics of Deformation and Flow of Particulate Materials,* C.S. Chang et al., Eds., published by ASCE, 1997.

[19] **Rowe, P.W.,** The stress-dilatancy relation for static equilibrium of an assembly of particles in contact, *Proc. Royal Soc.,* **A269**, 500–527, 1962.

[20] **Timoshenko, S.P. and Goodier, J.N.,** *Theory of Elasticity,* McGraw-Hill, 1951.

[21] **Sengara, I.W.,** *Finite Element and Experimental Study of Soil-Structure Interaction,* Ph.D. thesis, University of Wisconsin, 1992.

[22] **Lees, G.,** The measurement of particle shape and its influence in engineering materials, *J. Br. Granite Whinstone Fed.,* **4**, 1–22, 1964.